

**Molecular origins of adhesive failure: Siloxane elastomers pulled from a silica surface**Elizabeth M. Lupton,<sup>1</sup> Frank Achenbach,<sup>2</sup> Johann Weis,<sup>3</sup> Christoph Bräuchle,<sup>1</sup> and Irmgard Frank<sup>1,\*</sup><sup>1</sup>*Institute for Physical Chemistry, Center for Nanoscience and Department of Chemistry and Biochemistry, Ludwig Maximilians University Munich, Butenandtstrasse 5-13, 81377 Munich, Germany*<sup>2</sup>*Wacker Chemie AG, Werk Burghausen, 84480 Burghausen, Germany*<sup>3</sup>*Consortium für Elektrochemische Industrie, GmbH, Zielstattstrasse 20, 81379 Munich, Germany*

(Received 10 August 2006; revised manuscript received 28 March 2007; published 18 September 2007)

To gain insight into the molecular basis of failure processes in adhesives, we have performed a first-principles molecular dynamics study on siloxane oligomers adsorbed on a silica surface. We model covalent bond rupture in the high force regime of single molecule atomic force microscopy experiments where an elastomer is pulled from a substrate at constant velocity. Our system consists of covalent silicon-oxygen bonds which differ in the extent to which they are constrained by their location depending on whether they are in the elastomer, at the attachment or in the substrate. We find that the magnitude of the rupture force is dependent on whether the ruptured bond is in the polymer or at the attachment to the substrate. We determine a rupture force of 2.0 nN for an Si-O bond at the attachment when a polydimethylsiloxane hexamer is pulled from a  $\beta$ -cristobalite (100) slab.

DOI: 10.1103/PhysRevB.76.125420

PACS number(s): 68.37.Ps, 71.15.Pd, 81.40.Np, 82.35.Gh

**I. INTRODUCTION**

In this study we use first-principles molecular dynamics simulations to characterize the molecular origin of failure processes in siloxane adhesives. The binding of an adhesive to a substrate through specific chemical bonds and its resistance to degradation, either by mechanical fatigue or chemical attack from species in the environment, are factors which define the range of its applicability.<sup>1</sup> To assess the reliability of an adhesive, an understanding of the origins of material failure is required, in which bond rupture plays an important role. Here we investigate the response of an elastomer bound to a substrate to an applied tensile stress in order to understand the initiation of mechanical fatigue. The efficiency with which an adhesive polymer can distribute an applied stress throughout its backbone and into the substrate via the attachment by increasing bond lengths and angles is a major factor in determining the quality of the adhesive. Single molecule atomic force microscopy (AFM) experiments can probe the force required to stretch a single molecule between two surfaces until a bond in the system is ruptured giving a force curve characteristic of the molecule in the specified system.<sup>2,3</sup> Both classical and first-principles molecular dynamics simulations have been used in the past years to investigate theoretically the phenomena connected with stretching a molecular system and also the rupture processes.<sup>4-9,13-23</sup> The rupture force obtained, although associated with the rupture of one bond, is dependent on the system in which it finds itself and is affected by experimental parameters such as temperature, pulling rate,<sup>4,5</sup> solvent,<sup>6,7</sup> and the attachments to tip and substrate.<sup>8,9</sup> This method has primarily been applied to probing the strength of unspecific binding interactions in biological systems,<sup>10</sup> but also the force required to rupture a covalent bond has been measured.<sup>11,12</sup> The principle can therefore also be used to investigate synthetic materials where the response of the material to an applied stress and the rupture of specific bonds are important in their applications and to understand the underlying mechanisms which determine material strength. To

monitor how the force is transferred through systems such as those investigated in single molecule AFM experiments, we perform first-principles molecular dynamics simulations of pulling a molecule from a surface whereby the molecule and the substrate are described at the same level of theory throughout the simulation. This allows us to follow stress induced distortions and accurately describe the bond rupture process. We can distinguish between ultimate failure within the molecule, at the attachment, or within the substrate, and indicate which factors need to be modified in order to improve the performance of a material, for example, as an adhesive. In this study we concentrate specifically on the covalent bond breaking process in the high force regime of a single molecule AFM experiment (on the order of nN). We simulate the evolution of the electronic structure and consequent bond breaking of an oligomer pulled from a silica substrate to obtain a corresponding rupture force. As our focus is solely on covalent bond rupture, we do not investigate the entropy-determined polymer unfolding in the low force regime.

Siloxanes are used as adhesives, coatings, sealants, and lubricants in applications ranging from biomedical to aerospace.<sup>24</sup> The exceptional physical and chemical stability of polydimethylsiloxanes (PDMS) makes them reliable in diverse situations, but the origins of their ultimate failure is a problem where a study examining the response of single molecules can contribute to improving the material functionality. A previous study has experimentally examined the strength of hydrogen bonding of PDMS on a silica substrate,<sup>25</sup> and molecular dynamics studies have been applied to investigating stretching PDMS elastomers<sup>26,27</sup> and peeling them from a silica surface.<sup>27</sup> For the investigation of covalent bond rupture a quantum-mechanical description of the electronic structure is necessary. It has previously been shown with Car-Parrinello molecular dynamics (CPMD)<sup>28</sup> simulations that siloxane elastomers are highly flexible and that the bond lengths and angles increase simultaneously during stretching, with the Si-O-Si bond angle being able to take values up to 180°. Here we investigate how the applied

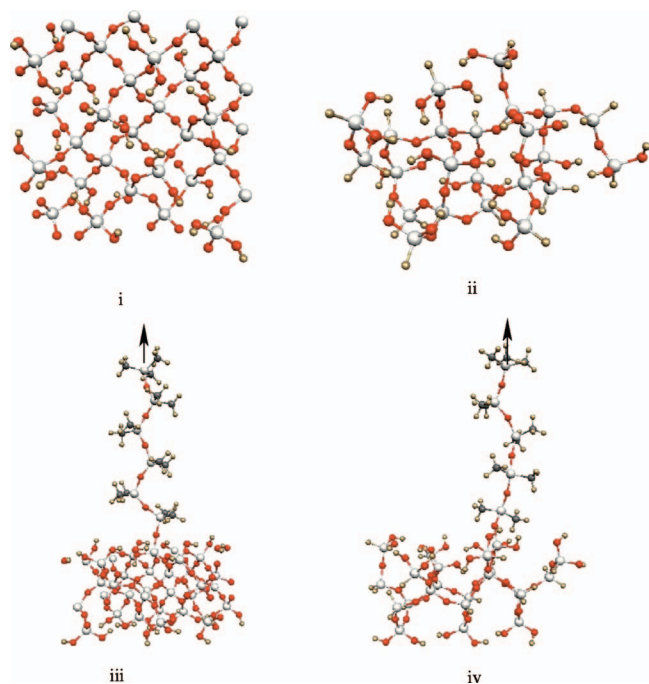


FIG. 1. (Color) The starting configurations for the calculations: grey, silicon; red, oxygen; black, carbon; yellow, hydrogen. (i) A top view of the  $\beta$ -cristobalite (100) surface slab, the structure is periodically repeated in the surface plane. The hydrogen bonded structures across the diagonal in the top layer are shown with the dashed lines. (ii) A top view of the surface cluster. (iii) A side view of the siloxane hexamer on the  $\beta$ -cristobalite (100) surface slab. The arrow indicates the pulling of the terminal silicon atom. (iv) The siloxane pentamer on the surface cluster. The arrow indicates the pulling of the terminal silicon atom.

tensile stress is transferred through a siloxane elastomer to a silica substrate by bending and stretching a series of covalent Si-O bonds, modeling a reduced system representing that investigated in AFM experiments. The system setup means that only a covalent Si-O bond can be ruptured, and we investigate where the weakest link in the system is and which factors lead to the concentration of stress at this point. We apply CPMD simulations to determine the evolution of the electronic structure “on the fly” during a molecular dynamics simulation, allowing a detailed description of mechanically induced bond rupture. Car-Parrinello simulations have previously been used to investigate pulling a molecule from a surface to form a nanowire, where a thiol molecule was pulled from a gold surface, extracting five gold atoms out of the surface before an Au-Au bond was ruptured.<sup>8</sup> In the present study the oriented covalent bonding in the substrate reduces the possibility of significant distortion of the silica surface as the siloxane molecule is pulled from the surface. We investigate polydimethylsiloxane oligomers adsorbed on cluster and slab representations of the  $\beta$ -cristobalite (100) surface with different pulling velocities. After detailing the setup for our simulations, we present the results showing how the systems respond to the applied tensile stress and which factors contribute to ultimate rupture. We then discuss the implications of our findings for the interpretation of AFM experiments and adhesive systems.

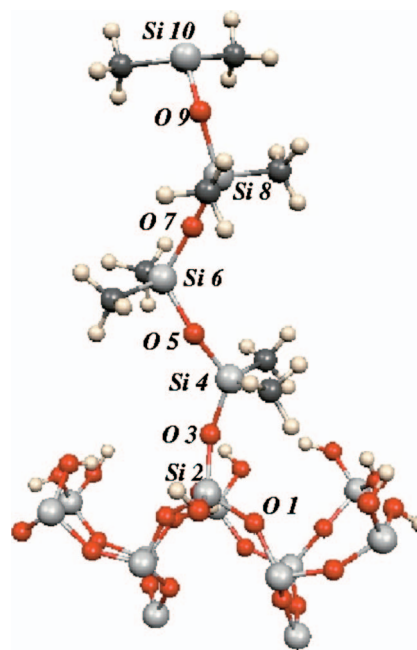


FIG. 2. (Color) A schematic diagram showing the attachment of the siloxane molecule to the substrate in detail. Color code: grey, silicon; red, oxygen; black, carbon; yellow, hydrogen. Only the central part of the simulated structure is shown. The  $O_3$ - $Si_4$  bond is the attachment bond and the labeling corresponds to that used in the discussion in the text.

## II. METHOD

We perform Car-Parrinello molecular dynamics simulations<sup>28,29</sup> where the electronic structure of the system is described using density-functional theory (DFT).<sup>30,31</sup> The Becke-Lee-Yang-Parr (BLYP) functional<sup>32,33</sup> is used for the electron exchange and correlation potential. The core electrons are described using the Troullier-Martins pseudopotentials<sup>34</sup> and the Kohn-Sham orbitals are expanded using a plane-wave basis set with a cutoff of 70 Ry. We determine the electronic structure at the  $\Gamma$  point of the unit cell. In a previous study on isolated siloxanes,<sup>5</sup> we did not observe radical formation during bond rupture in any of the simulations and so we use the spin-restricted BLYP functional here. All molecular dynamics simulations are performed with a time step of 0.1 fs at 300 K and a fictitious electron mass of 400 atomic units.

We perform two types of simulations: one in which a siloxane pentamer (five silicon atoms in the backbone) is pulled from a cluster representation of the  $\beta$ -cristobalite (100) surface; and the other in which a siloxane hexamer (six silicon atoms in the backbone) is pulled from a slab representation of the surface, where the surface cell is periodically repeated in the surface plane (Fig. 1). A detail of the attachment structure is shown in Fig. 2, highlighting the covalent bond between the siloxane and the substrate in the simulations.

We first determine the equilibrium geometry of the (100) surface without adsorbed siloxane by cleaving the bulk  $\beta$ -cristobalite to give four silicon layers and saturating the terminal oxygen atoms with hydrogens (Fig. 1), as would be

the state of the exposed silica surface in the experiment. We used a periodically repeating unit cell of  $14.3 \times 14.3 \text{ \AA}$  in the surface plane and  $16.0 \text{ \AA}$  perpendicular to the surface, separating the slabs by  $5.5 \text{ \AA}$  in the direction perpendicular to the surface. We relaxed all atomic positions and equilibrated the structure for 1 ps at 300 K. After 0.5 ps we found no further change in the structure, and obtained the same hydrogen bonding network on the surface as Iarlori *et al.*<sup>35</sup> in their CPMD study of the  $\beta$ -cristobalite (100) surface.

The starting geometry for the cluster simulations was obtained by trimming the silica slab, saturating the terminal silicon and oxygen atoms of the cluster with hydrogens, and covalently attaching a siloxane pentamer on top with the molecular axis perpendicular to the surface plane (Fig. 1). Such an attachment to the substrate is proposed for AFM experiments designed to investigate the strength of covalent interactions. The starting geometry of the siloxane pentamer is taken from its equilibrated structure at 300 K determined using CPMD. The cluster has three silicon surface layers, with eight silicon atoms in the uppermost layer and three silicon atoms in the lowest layer. A cell of  $20.1 \times 16.0 \text{ \AA}$  in the surface plane and  $29.0 \text{ \AA}$  perpendicular to the surface was used. In order to obtain the initial configuration, we equilibrated the system for 200 fs at 300 K, keeping the positions of the terminal silicon atom of the pentamer furthest from the surface and the silicon atoms in the lowest layer of the cluster fixed. The resulting structure was used as the initial configuration for the rupture simulations. This represents one possible stable configuration for the system at 300 K, at a point where all the Si-O bond lengths are clearly below the breaking point. We then move the terminal silicon atom of the pentamer by a fixed amount away from the surface for each time step to cause stretching of the molecule at constant velocity. This simulates the way in which a tensile stress is applied in experiments.<sup>36</sup> Hence we fully include entropy effects on the time scale of the simulation which however is significantly shorter than the time scale of single molecule experiments. We performed two different simulations, one with a pulling velocity of 273 m/s and one with a velocity of 55 m/s. These pulling velocities permit a first-principles molecular dynamics simulation of the extension and rupture process, but are greater than experimental pulling velocities which are typically on the order of  $10^{-6}$  m/s. We have previously discussed the influence of elevated pulling velocities on rupture in the case of carbon-based polymers<sup>4</sup> and siloxanes.<sup>5</sup>

In the slab simulations a siloxane hexamer is covalently attached to the slab with an average Si-O bond length in the hexamer of  $1.67 \text{ \AA}$ . We use cell dimensions of  $14.3 \times 14.3 \text{ \AA}$  in the surface plane and  $32.0 \text{ \AA}$  perpendicular to the surface plane. After equilibrating the starting geometry for 200 fs at 300 K with the silicon atoms in the lowest layer of the surface and the terminal silicon atom in the hexamer furthest from the surface fixed, we move the terminal silicon atom in the hexamer by a predefined amount away from the surface for each time step to stretch the molecule. In the first part of the simulation, a pulling rate of 55 m/s was used and this was then increased to 273 m/s to observe bond rupture.

### III. THE SILOXANE PENTAMER ON A CLUSTER REPRESENTATION OF THE $\beta$ -CRISTOBALITE (100) SURFACE

We pull a siloxane pentamer from a cluster representation of the  $\beta$ -cristobalite (100) surface until an Si-O bond in the system is ruptured. For the simulation at 273 m/s, we start from a fully relaxed geometry with an average Si-O bond length of  $1.67 \text{ \AA}$  in the pentamer, and for the simulation at 55 m/s we start from a prestretched system with a corresponding average Si-O bond length of  $1.76 \text{ \AA}$ .

In the first simulation at 273 m/s bond rupture occurs in the siloxane pentamer, but in the second simulation at 55 m/s the Si-O (Fig. 2  $O_3$ - $Si_4$ ) bond of the attachment is ruptured. The different stages of the simulations are shown in snapshots in Figs. 3 and 4 with the corresponding energy curves. From the snapshots it can be seen that in both simulations the pentamer is stretched out before rupture, with the oxygen and silicon atoms belonging to the surface at the attachment pulled out, causing a local deformation in the substrate. The recoil of the fragments as the bond lengths and angles relax after rupture is apparent in the last snapshot. The energy increases as the pentamer is stretched and the rupture force can be taken from the gradient of the energy curves before the bond is broken. The rupture force is 4.5 nN for the simulation at 273 m/s and 3.5 nN for the simulation at 55 m/s corresponding to the breaking of a bond within the siloxane and at the attachment, respectively.

The qualitative difference between the outcomes of the simulations, where different Si-O bonds are broken, can be assessed by examining the response of the molecule to being stretched by increasing bond lengths and angles. In examining these structural changes as the molecule is stretched, we need to consider three parameters: the Si-O bond lengths, and the Si-O-Si and O-Si-O bond angles — in three different environments: the siloxane hexamer, the attachment, and the  $\beta$ -cristobalite surface. The flexibility of the siloxanes has been demonstrated in studies of isolated molecules under tensile stress,<sup>5</sup> but the bond lengths and angles in the cluster are more constrained. The bonds which are stretched by the applied force are all covalent and differ only in the extent in which they are constrained in their environment.

During the first part of the simulation at 273 m/s, the average bond lengths and angles in the pentamer increase steadily from  $1.67$  to  $1.75 \text{ \AA}$ , the attachment bond (Fig. 2,  $O_3$ - $Si_4$ ) increases from  $1.67$  to  $1.77 \text{ \AA}$ , and the bond lengths in the cluster remain constant at  $1.65 \text{ \AA}$ . The oxygen atom in the cluster at the attachment (Fig. 2,  $O_3$ ) is pulled out of the surface plane and the silicon atom below it (Fig. 2,  $Si_2$ ) is pulled into the uppermost surface layer. The applied stress is therefore distributed by stretching the pentamer, extending the attachment, and a local deformation of the surface in the first part of the simulation.

Bond lengths and angles for the last part of the simulation at 273 m/s and for the simulation at 55 m/s are shown in Fig. 5. In both simulations the Si-O bonds in the pentamer (Fig. 2,  $O_7$ - $Si_8$ ) and at the attachment (Fig. 2,  $O_3$ - $Si_4$ ) increase before rupture. Although the Si-O bond length in the surface (Fig. 2,  $O_1$ - $Si_2$ ) remains roughly constant, the Si-O bonds in the pentamer and at the attachment are longer and

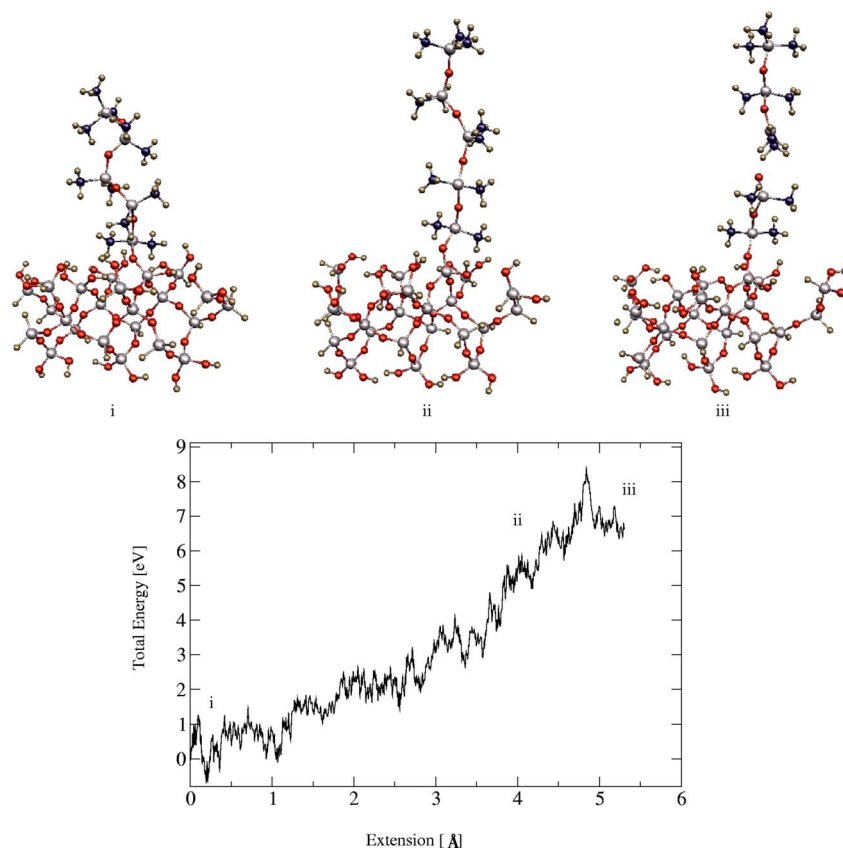


FIG. 3. (Color online) Snapshots of the simulation pulling a siloxane pentamer from a cluster representation of the  $\beta$ -cristobalite (100) surface with a pulling rate of 273 m/s and the corresponding energy curve. The different stages of the simulation (i) start, (ii) during, and (iii) after rupture are indicated on the energy curve. The energy increases as the terminal silicon atom of the pentamer is pulled away from the surface. The siloxane is fully stretched with limited distortion of the substrate when an Si-O bond in the elastomer backbone breaks.

more flexible than those in the substrate. There are differences between the two simulations in the Si-O-Si bond angles in the pentamer and at the attachment. The Si-O-Si bond angles in the second simulation are greater than those in the first simulation and can take values up to  $180^\circ$ . In the second simulation, the oxygen and silicon atoms in the cluster are pulled further out of the surface than in the first simulation. The oxygen atom at the attachment is pulled a total of  $1.7 \text{ \AA}$  out of the surface from the equilibrated starting geometry and the silicon atom by  $1.3 \text{ \AA}$ , compared to  $1.5 \text{ \AA}$  and  $1.0 \text{ \AA}$  in the first simulation, respectively. This reflects the fact that lower pulling velocities allow for more pronounced structural rearrangements.

#### IV. THE SILOXANE HEXAMER ON $\beta$ -CRISTOBALITE (100)

We simulate pulling a siloxane molecule from a  $\beta$ -cristobalite (100) slab by moving the terminal silicon atom of the siloxane hexamer away from the surface at a fixed rate. We start with an unstretched siloxane hexamer (Si-O,  $1.67 \text{ \AA}$ ) covalently attached to a surface oxygen atom. We then stretch the elastomer at a rate of 55 m/s to guarantee good relaxation of the extended structure. After stretching for 2.5 ps, corresponding to an extension of  $1.3 \text{ \AA}$ , the rate was

increased to 273 m/s and stretched for 0.3 ps corresponding to an extension of  $1.7 \text{ \AA}$  until bond rupture occurred.

The increase in total energy with increasing extension is shown in Fig. 6 with snapshots from the simulation. The energy increases steadily until rupture occurs at the attachment. The rupture force, taken from the gradient of the energy curve, amounts to 2.0 nN. From the snapshots it can be seen that the applied stress primarily results in stretching the elastomer with a local distortion of the substrate, as in the cluster calculations.

The Si-O bond lengths, Si-O-Si, and O-Si-O angles, have a degree of flexibility in the siloxane elastomers but are restricted in the  $\beta$ -cristobalite slab. In the first part of the simulation, the surface Si-O bond lengths have the lowest average value of  $1.64 \text{ \AA}$ , the average Si-O bond in the hexamer is  $1.68 \text{ \AA}$ , and  $1.72 \text{ \AA}$  is the average length of the attachment bond. The Si-O bond neighboring the attachment in the surface (Fig. 2, Si<sub>2</sub>-O<sub>3</sub>) is slightly elongated at  $1.65 \text{ \AA}$  compared to the average surface value, and the neighboring Si-O bond in the hexamer (Fig. 2, Si<sub>4</sub>-O<sub>5</sub>) is shorter at  $1.67 \text{ \AA}$  than the elastomer average. No significant change in the average values of the bond lengths is observed in this first phase of the simulation at 55 m/s. There is also no change in the average O-Si-O angle in any part of the system. The only increase in any of the bond angles is that of the Si-O-Si bond angle at the attachment, whose average value increases from  $140^\circ$  to



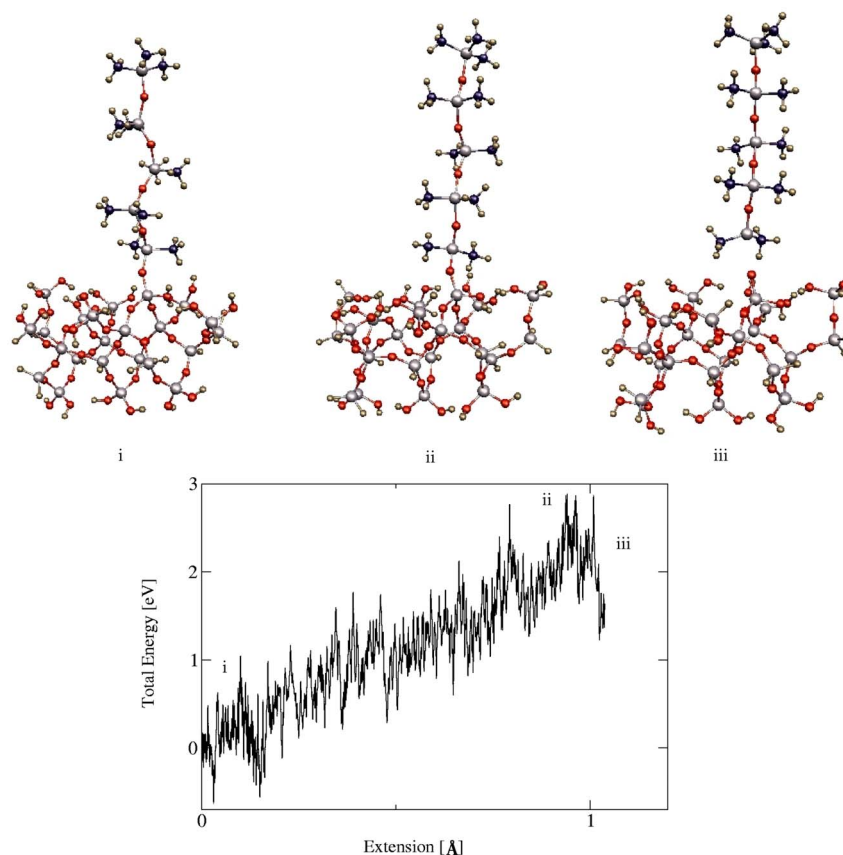


FIG. 4. (Color online) Snapshots of the simulation pulling a siloxane pentamer from a cluster representation of the  $\beta$ -cristobalite (100) surface with a pulling rate of 55 m/s and the corresponding energy curve. The different stages of the simulation (i) start (the system has already been prestretched), (ii) during, and (iii) after rupture are indicated on the energy curve. The attachment is more strained compared to the simulation at 273 m/s and it is this Si-O bond which ultimately breaks.

160°. It has already been noted that the siloxane Si-O-Si bond angle is highly flexible, so it is not surprising that as the molecule is pulled from the surface it is this parameter which is distorted the most. The other notable change in the system is that the surface oxygen atom at the attachment is raised by 0.7 Å out of the surface layer, and the silicon atom in the layer below is raised by 0.5 Å into the uppermost surface layer. No other significant structural distortions occur in the system.

To examine the rupture process, we increased the pulling rate to 273 m/s. During this part of the simulation we pulled a further 1.7 Å, the bond lengths and angles from the last part of the simulation before rupture are shown in Fig. 7. The Si-O bond in the slab (Fig. 2, O<sub>1</sub>-Si<sub>2</sub>) has the lowest bond length and is not as affected as the other bonds in the system, as was the case in the first part of the simulation. The Si-O bonds at the attachment (Fig. 2, O<sub>3</sub>-Si<sub>4</sub>) and in the hexamer (Fig. 2, O<sub>7</sub>-Si<sub>8</sub>) only increase significantly just before rupture, where they are elongated by up to 0.2 Å. The greatest change occurs in the Si-O-Si bond angle at the attachment (Fig. 2, Si<sub>2</sub>-O<sub>3</sub>-Si<sub>4</sub>) which is effectively pulled straight. The bond lengthening and increase in the Si-O-Si angle indicate that it is the attachment which is most destabilized by the applied stress.

During the complete simulation the terminal silicon atom of the hexamer is pulled a total of 2.8 Å until the Si-O bond

at the attachment (Fig. 2, O<sub>3</sub>-Si<sub>4</sub>) is ruptured. The greatest change in the system occurs for the Si-O-Si bond angle (Fig. 2, Si<sub>2</sub>-O<sub>3</sub>-Si<sub>4</sub>) at the attachment which increases from 140° in the equilibrated starting structure to 180° at the point of rupture. No structural distortion of the surface involving bond rearrangements occurs during the simulation, but the surface oxygen bound to the hexamer is pulled a total of 1.2 Å out of the surface plane, and the silicon beneath it by 0.8 Å into the uppermost surface layer. These atoms relax back into the surface after rupture but do not retain their original positions on the time scale of the simulation. The distortion does not penetrate into the surface: the second layer silicon atoms are not significantly displaced. The simulation indicates that it is the attachment which is most likely to be ruptured with limited distortion to the substrate as the hexamer is pulled away.

Note that “breaking at the attachment” as observed in the present study does not mean breaking of a chemically weaker bond. The bond that is breaking (Si<sub>4</sub>-O<sub>3</sub>) is a normal Si-O bond with both atoms having the same neighbors as the other silicon and oxygen atoms within the polymer chain (in contrast to, for example, Si<sub>2</sub> which is part of the cristobalite network). The destabilization leading to the opening of the Si-O-Si angle (Fig. 7) is of a mechanical, not chemical, nature.

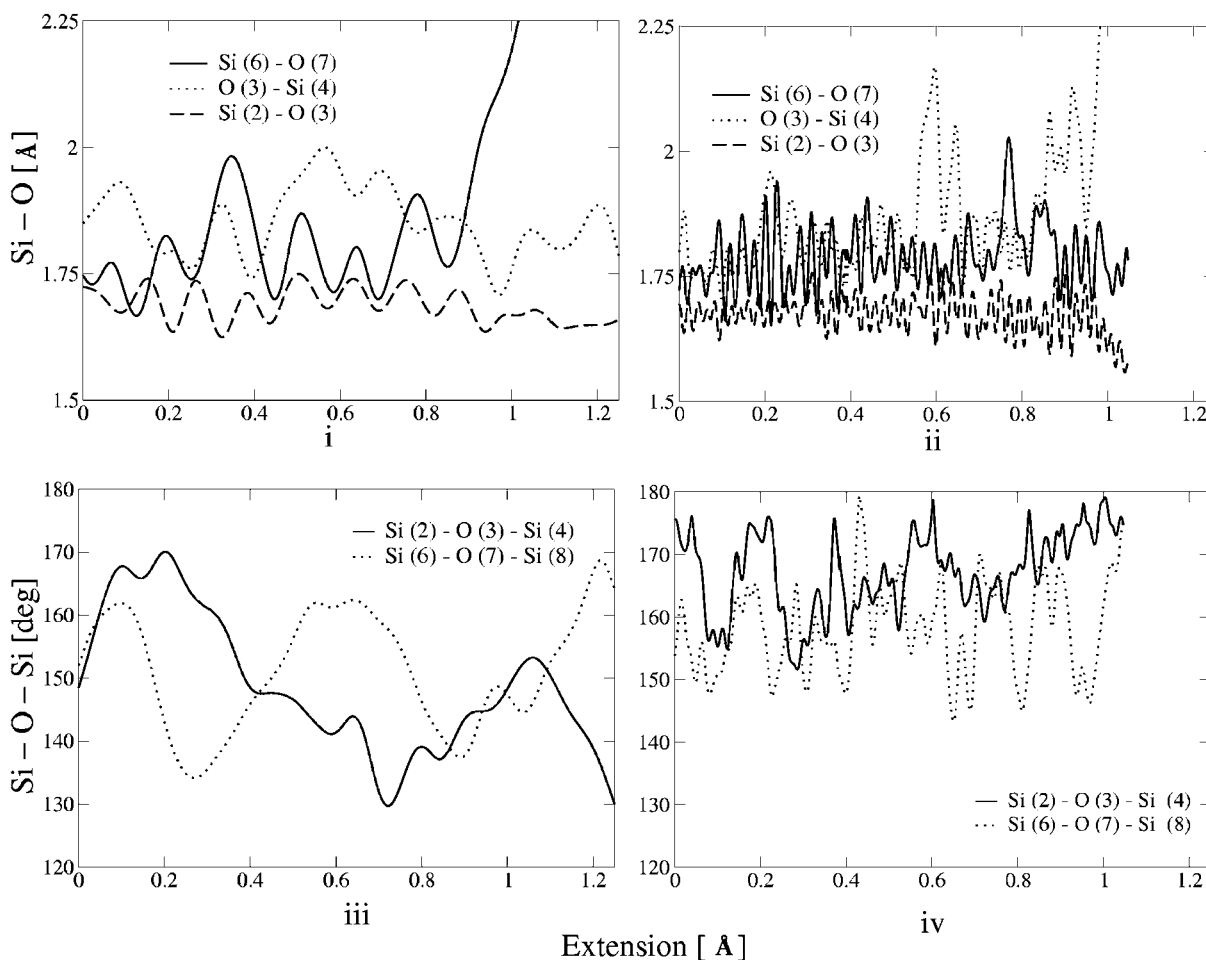


FIG. 5. The relevant bond lengths and angles for the siloxane hexamer on a  $\beta$ -cristobalite (100) surface cluster. The Si-O bond lengths for (i) the simulation at 273 m/s and (ii) the simulation at 55 m/s. In both cases the atom numbering corresponds to that shown in the schematic diagram in Fig. 2. The Si-O-Si bond angle at the attachment and for an Si-O-Si linkage in the siloxane chain for (iii) the simulation at 273 m/s and (iv) the simulation at 55 m/s. Again the atom numbering corresponds to that in Fig. 2. By comparing the bond lengths of the different simulations, it can be seen that the attachment bond in the simulation at 55 m/s is clearly destabilized at the end of the simulation, whereas this is not the case for the higher pulling rate. The Si-O-Si bond angles can take values up to  $180^\circ$  in the simulation at 55 m/s.

## V. COMPARISON OF RUPTURE FORCES

The strength of a chemical bond, as defined by the force required to break it, is influenced by characteristics of the specific system such as the temperature, the pulling rate, and the nature of the chemical bond itself. In this study we have concentrated on how different parts of the system can be deformed as a molecule is pulled from a surface and the rupture force associated with bonds ruptured at different points in the system. In all simulations a siloxane elastomer is pulled from the surface, the molecule is stretched out and the silica substrate is deformed locally at the attachment. The Si-O bond lengths and angles increase within the elastomer and at the attachment, and the oxygen and silicon atoms at the attachment and in the substrate are pulled out of the surface. In one simulation it is an Si-O bond in the siloxane elastomer which is ruptured and in two simulations it is the attachment bond which is broken. We determine the rupture force associated with rupture of a specific Si-O bond *within*

*the system*, which includes the attachment of the siloxane to the silica surface, by taking the maximum of a numerical differentiation of the energy curve up to the rupture point. For the siloxane pentamer attached to the cluster representation of the  $\beta$ -cristobalite (100) surface, a rupture force of 4.5 nN is determined for rupture within the siloxane. The rupture force in CPMD simulations of Si-O bond rupture within an isolated siloxane decamer is 4.4 nN reported in Ref. 5, suggesting that if rupture occurs within the elastomer, the rupture force is not influenced by attaching the elastomer to the substrate. For the other two simulations where the attachment bond is broken, a lower rupture force is obtained. In the second calculation with the cluster representation of the surface, a force of 3.5 nN is obtained, which is significantly lower than that determined from simulations where a bond within the siloxane molecule is ruptured. For the siloxane attached to a  $\beta$ -cristobalite (100) slab we obtain a rupture force for the attachment bond of 2.0 nN which lies in the range reported for covalent bond rupture of  $2.0 \pm 0.3$  nN.<sup>11</sup>

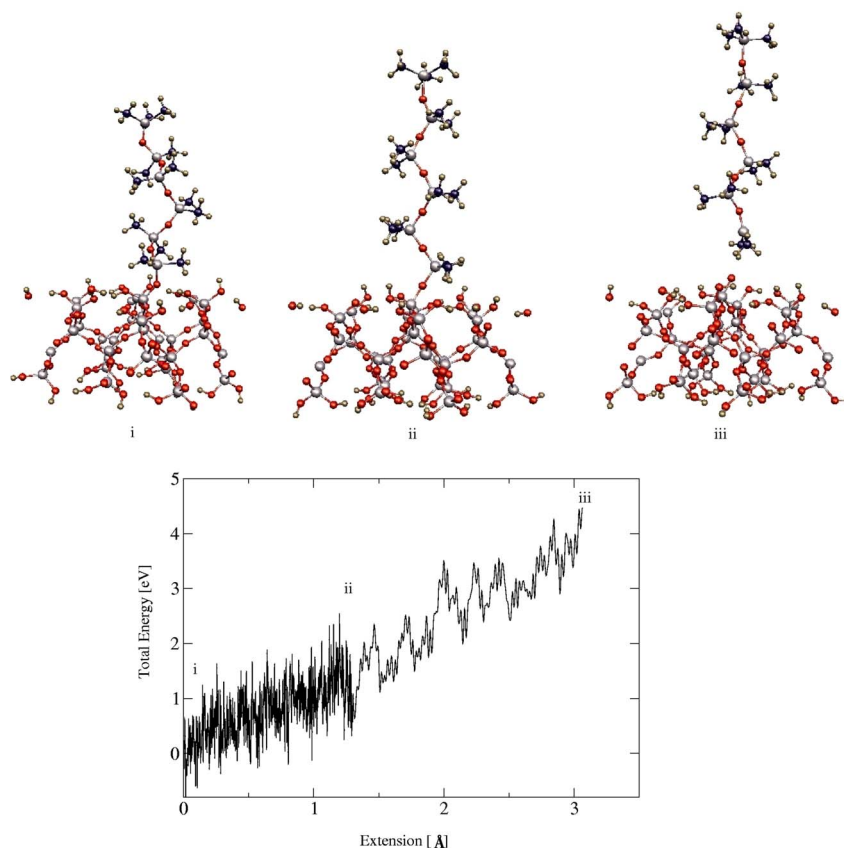


FIG. 6. (Color online) Snapshots of the simulation pulling a siloxane hexamer from a slab representation of the  $\beta$ -cristobalite (100) surface and the corresponding energy curve. Up to an extension of 1.3 Å the pulling rate is 55 m/s, thereafter the rate is 273 m/s. The different stages of the simulation (i) start, (ii) during, and (iii) after rupture are indicated on the energy curve. The energy increases as the terminal silicon atom of the hexamer is pulled away from the surface. The elastomer is stretched out before rupture occurs at the attachment.

We predict that on repeated simulations over the same range of pulling velocities we would obtain bond rupture at different points in the system, but conclude that the rupture force associated with the attachment will always be significantly lower than that within the siloxane molecule. These results therefore indicate that the location of the Si-O bond affects the magnitude of the rupture force. Our findings correspond to the interpretation of the low experimental rupture force for a polymer with a S-Au attachment to a gold surface [ $1.4 \pm 0.3$  nN (Ref. 11)] using CPMD simulations<sup>8</sup> where ultimately an Au-Au bond was broken.

This outcome shows that it is not just the nature of the specific bond which determines the magnitude of the rupture force, but the position of the rupturing bond within the system is just as important. In the case of the siloxane molecule on a silica surface, the attachment acts as a barrier between a part of the system where additional energy is easily distributed (the molecule), and where the atoms are constrained (the substrate). The attachment itself can be flexible, mainly by increasing the Si-O-Si angle which is not constrained during the simulations. Although the attachment is flexible, it is bound to the rigid network of the substrate where the increase in energy cannot easily be further distributed by increasing bond lengths and angles.

We emphasize that the computed value of 2.0 nN is connected with a large uncertainty mainly originating from the

use of too high pulling velocities and a too short polymer chain. Both effects should lower the theoretical value to some degree.<sup>5</sup> Side reactions such as hydrolysis<sup>7</sup> may reduce the effectively measured rupture force. In comparison, the uncertainty introduced by the use of the density-functional approximation should be relatively small. The uncertainty due to the use of the Car-Parrinello molecular dynamics formalism is negligible as the Born-Oppenheimer approximation holds throughout the reaction. Finally, we are not able to perform many simulations in order to get good statistics. From all these effects, we estimate that our computed rupture force is connected with an uncertainty no greater than  $\pm 0.5$  nN for comparison with single molecule AFM experiments. Hence, while the numerical agreement with the experimental value is to some degree fortuitous, our calculations clearly demonstrate the strong influence of the surface.

## VI. CONCLUSIONS

We have used Car-Parrinello molecular dynamics simulations to characterize covalent bond rupture when a siloxane oligomer is pulled from a silica surface. We find a force of 2.0 nN for rupture of a covalent Si-O bond at the attachment of the elastomer to the substrate. The simulations model the covalent bond rupture process as examined in single mol-

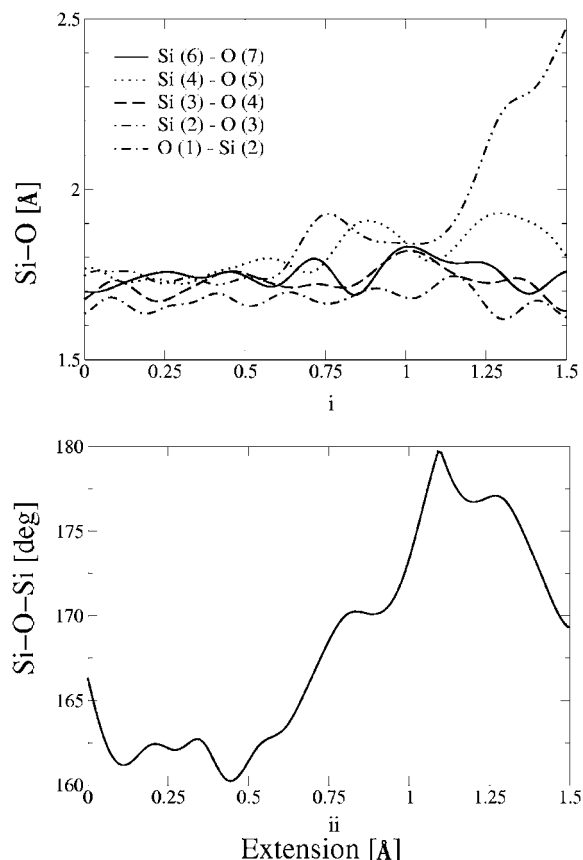


FIG. 7. Bond rupture from the  $\beta$ -cristobalite (100) slab for the last part of the simulation at 273 m/s. (i) The Si-O bond lengths. The numbering corresponds to that shown in the schematic diagram in Fig. 2. (ii) The Si-O-Si bond angle at the attachment. The bond lengths of the attachment and the elastomer increase just before rupture. The Si-O-Si angle at the attachment is effectively pulled straight before rupture.

ecule AFM experiments where an elastomer is pulled from a substrate by an AFM tip at constant velocity. In our system there are only covalent silicon-oxygen bonds which differ in the extent to which they are constrained by their surroundings: there are no obvious sacrificial bonds. The numerical accuracy of our approach is mainly limited by the use of comparatively high pulling velocities and by the lack of statistics. Nevertheless we show that if a bond is ruptured within the elastomer, the magnitude of the rupture force is significantly greater than that associated with rupture at the attachment which is closer to the experimentally reported value. We propose that the rupture forces reported in AFM experiments are not only determined by the specific nature of the chemical bond, but the environment of the rupturing bond is also important.

We have found bond rupture both within the elastomer and at the attachment corresponding to adhesive and cohesive failure, respectively. In these simulations examining single molecules, we only observe elastic deformation before rupture, with no bonds affected apart from the broken bond, which is in contrast to the results that have been obtained in CPMD simulations for the easily deformed gold surface where the formation of gold nanowires from a step edge was observed. Our simulations emphasize the importance of considering the environment, in addition to the nature of the chemical bond, in describing the molecular origins of adhesive failure.

#### ACKNOWLEDGMENTS

This work is funded through the VW-Stiftung, the DFG (SFB 486 “Manipulation von Materie auf der Nanometerskala”) and Wacker Chemie AG, and we gratefully acknowledge the John von Neumann Institute for Computing in Jülich (project hmu101) and the Leibniz-Rechenzentrum Munich (project h0622) for computer time.

\*frank@cup.uni-muenchen.de

<sup>1</sup>A. Baldan, *J. Mater. Sci.* **39**, 4729 (2004).

<sup>2</sup>T. Hugel and M. Seitz, *Macromol. Rapid Commun.* **22**, 989 (2001).

<sup>3</sup>A. Janshoff, M. Neitzert, Y. Oberdörfer, and H. Fuchs, *Angew. Chem., Int. Ed.* **39**, 3212 (2000).

<sup>4</sup>U. F. Röhrig and I. Frank, *J. Chem. Phys.* **115**, 8670 (2001).

<sup>5</sup>E. M. Lupton, C. Nonnenberg, I. Frank, F. Achenbach, J. Weis, and C. Bräuchle, *Chem. Phys. Lett.* **414**, 132 (2005).

<sup>6</sup>D. Aktah and I. Frank, *J. Am. Chem. Soc.* **124**, 3402 (2002).

<sup>7</sup>E. M. Lupton, F. Achenbach, J. Weis, C. Bräuchle, and I. Frank, *J. Phys. Chem. B* **110**, 14557 (2006).

<sup>8</sup>D. Krüger, H. Fuchs, R. Rousseau, D. Marx, and M. Parrinello, *Phys. Rev. Lett.* **89**, 186402 (2002).

<sup>9</sup>D. Krüger, R. Rousseau, H. Fuchs, and D. Marx, *Angew. Chem.* **42**, 2251 (2003).

<sup>10</sup>H. Clausen-Schaumann, M. Seitz, R. Krautbauer, and H. E. Gaub, *Curr. Opin. Chem. Biol.* **4**, 524 (2000).

<sup>11</sup>M. Grandbois, M. Beyer, M. Rief, H. Clausen-Schaumann, and H. E. Gaub, *Science* **283**, 1727 (1999).

<sup>12</sup>M. A. Lantz, H. J. Hug, R. Hoffmann, P. J. A. van Schendel, P. Kappenberger, S. Martin, A. Baratoff, and H. J. Güntherodt, *Science* **291**, 2580 (2001).

<sup>13</sup>H. Grubmüller, B. Heymann, and P. Tavan, *Science* **271**, 997 (1996).

<sup>14</sup>B. Heymann and H. Grubmüller, *Chem. Phys. Lett.* **307**, 425 (1999).

<sup>15</sup>B. Heymann and H. Grubmüller, *Phys. Rev. Lett.* **84**, 6126 (2000).

<sup>16</sup>M. Rief and H. Grubmüller, *ChemPhysChem* **3**, 255 (2002).

<sup>17</sup>S. Izrailev, S. Stepaniants, M. Balsera, Y. Oono, and K. Schulten, *Biophys. J.* **72**, 1568 (1997).

<sup>18</sup>B. Isralewitz, M. Gao, and K. Schulten, *Curr. Opin. Struct. Biol.* **11**, 224 (2001).

<sup>19</sup>M. V. Bayas, K. Schulten, and D. Leckband, *Biophys. J.* **84**, 2223 (2003).



- <sup>20</sup>A. M. Saitta, P. D. Soper, E. Wasserman, and M. L. Klein, *Nature* (London) **399**, 46 (1999).
- <sup>21</sup>A. M. Saitta and M. L. Klein, *J. Chem. Phys.* **111**, 9434 (1999).
- <sup>22</sup>A. M. Saitta and M. L. Klein, *J. Phys. Chem. B* **104**, 2197 (2000).
- <sup>23</sup>A. M. Saitta and M. L. Klein, *J. Phys. Chem. B* **105**, 6495 (2001).
- <sup>24</sup>*Organosilicon chemistry: From molecules to materials* IV–VI, edited by N. Auner and J. Weis (VCH, Weinheim, 2000–2005).
- <sup>25</sup>T. J. Senden, J. M. di Meglio, and P. Auroy, *Eur. Phys. J. B* **3**, 211 (1998).
- <sup>26</sup>J. S. Smith, D. Bedrov, and G. D. Smith, *Macromolecules* **38**, 8101 (2005).
- <sup>27</sup>D. E. Hanson, *J. Chem. Phys.* **113**, 7656 (2000).
- <sup>28</sup>R. Car and M. Parrinello, *Phys. Rev. Lett.* **55**, 2471 (1985).
- <sup>29</sup>CPMD code, Copyright IBM Corp. 1990–2006, Copyright MPI für Festkörperforschung Stuttgart 1997–2001.
- <sup>30</sup>P. Hohenberg and W. Kohn, *Phys. Rev. B* **136**, 864 (1964).
- <sup>31</sup>W. Kohn and L. J. Sham, *Phys. Rev.* **140**, A1133 (1965).
- <sup>32</sup>A. D. Becke, *Phys. Rev. A* **38**, 3098 (1988).
- <sup>33</sup>C. Lee, W. Yang, and R. G. Parr, *Phys. Rev. B* **37**, 785 (1988).
- <sup>34</sup>N. Troullier and J. L. Martins, *Phys. Rev. B* **43**, 1993 (1991).
- <sup>35</sup>S. Iarlori, D. Ceresoli, M. Bernasconi, D. Donadio, and M. Parrinello, *J. Phys. Chem. B* **105**, 8007 (2001).
- <sup>36</sup>E. Evans and K. Ritchie, *Biophys. J.* **72**, 1541 (1997).